Cancer Cell International

RESEARCH

Open Access

Integrated lipidomics and RNA-seq reveal prognostic biomarkers in well-differentiated and dedifferentiated retroperitoneal liposarcoma

Xiaopeng Wang[1†], Jingjing Ye[2†], Yan Wu[3], Hongtao Zhang[4], Chengpeng Li[1], Bonan Liu[1], Xiaoya Guan[1], Xiuyun Tian[1], Weiwei Jia[1], Qiao Liu[1], Shuquan Li[1], Rongze Sun[1], Daoning Liu[1], Guoqiang Xue[1], Zhen Wang[1], Liang Yan[1], Ang Lv[1], Jianhui Wu[1], Hui Qiu[1*] and Chunyi Hao[1*]

Abstract

Background Retroperitoneal liposarcoma (RLPS) is a mesenchymal malignant tumor characterized by different degrees of adipocytic differentiation. Well-differentiated liposarcoma (WDLPS) and dedifferentiated liposarcoma (DDLPS) are two of the most common subtypes of RLPS, exhibiting clear differences in biological behaviors and clinical prognosis. The metabolic features and genomic characteristics remain unclear.

Methods This study employed lipidomic and RNA-seq analyses of RLPS tissues from 19 WDLPS and 29 DDLPS patients. Western blot and immunohistochemistry staining were performed to verify the tumor tissue protein levels of TIMP1, FN1, MMP11, GPNMB, and ECM1. Enzyme-linked immunosorbent assay (ELISA) was performed to evaluate different serum protein levels in 128 blood samples from patients with RLPS. Multivariate analysis was performed to identify the most crucial variables associated with overall survival (OS) and recurrence-free survival (RFS) of the RLPS patients.

Results Lipidomic analysis revealed a significant difference in lipid metabolism, particularly in phosphatidylcholines and triacylglycerides metabolism. RNA sequencing analysis revealed that 1,630 differentially expressed genes (DEGs) were significantly enriched in lipid metabolism, developmental process, and extracellular matrix (ECM) pathways. Integrated lipidomic and transcriptomic analysis identified 29 genes as potential biomarkers between WDLPS and DDLPS. Among the 29 DEGs, we found that TIMP1, FN1, MMP11, GPNMB, and ECM1 were increased in DDLPS tumor tissues than in WDLPS tumor tissues. The receiver operating characteristic (ROC) curve showed high specificity and sensitivity in diagnosing patients using a five-gene combination (AUC = 0.904). ELISA revealed a significant increase

†Xiaopeng Wang and Jingjing Ye contributed equally to this work.

*Correspondence:
Hui Qiu
qiuhui@bjmu.edu.cn
Chunyi Hao
haochunyi@bjmu.edu.cn

Full list of author information is available at the end of the article

in the serum levels of ECM1 and GPNMB in patients with DDLPS compared to patients with WDLPS. ECM1 increased progressively across different FNCLCC Grades, correlating negatively with RFS ($P=0.043$). GPNMB levels showed a negative correlation with OS ($P=0.019$).

Conclusions Our study reveals different lipid metabolism, several transcriptional pathways between WDLPS and DDLPS, and examines several serum markers associated with the prognosis of RLPS. These findings provide a vital basis for future endeavors in diagnosing and predicting the prognosis of retroperitoneal liposarcoma with different differentiations.

Keywords Retroperitoneal liposarcoma, Biomarker, Lipidomics, RNA sequencing

Introduction

Liposarcoma (LPS) is a mesenchymal malignant tumor characterized by a heterogeneous class of adipocytic differentiation. It comprises approximately 24% of extremity soft tissue sarcomas and 45% of soft tissue sarcomas in retroperitoneum [1]. RLPS usually exhibits a poorer prognosis compared with their counterparts located in the extremities [2]. Liposarcoma can be categorized into the following five main subtypes based on the WHO classification: atypical lipomatous tumor or well-differentiated liposarcoma, dedifferentiated liposarcoma, myxoid liposarcoma, pleomorphic liposarcoma, and myxoid pleomorphic liposarcoma [3]. WDLPS and DDLPS are the most common types, accounting for approximately 90% of retroperitoneal liposarcomas and exhibiting different biological behaviors and clinical prognoses [2, 4]. DDLPS exhibits a higher occurrence of local recurrence and distant metastasis than WDLPS, which exhibits minimal distant metastasis [5]. DDLPS mostly arises as a focal growth within precursor WDLPS lesions [2, 6, 7]. Presently, surgery is the only potentially curable treatment. However, due to the significant size of the tumor and its infiltration into nearby important organs and blood vessels, complete resection is difficult [8]. Chemotherapy and radiotherapy have shown limited effectiveness in improving patient survival [9, 10]. Furthermore, immunotherapy and targeted therapy require large-scale preclinical studies and clinical trials to evaluate the efficacy and safety [11–14]. Many classical genomic analyses have consistently revealed Chr12q amplification, encompassing key genes encoding MDM2, CDK4, and HMGA2, as pivotal in the development of WDLPS and DDLPS [1, 2, 15, 16]. Despite these insights, the metabolic features and genomic characteristics remain unclear, and reliable prognostic biomarkers are elusive.

Abnormal lipid metabolism and lipid metabolic reprogramming are closely related to cell signal transduction, drug resistance, immune microenvironment adaptation and other processes; These factors are thought to play important roles in the occurrence and development of tumors [17–19]. Zhou et al. compared the lipid profiles of WDLPS and DDLPS using the LC-MS/MS method. They found that WDLPS contains a large numbers of neutral lipid components, such as triglycerides and diacylglycerols, whereas DDLPS is composed of more phospholipids, such as phosphocholines (PCs), phosphoethanolamines (PEs), and sphingomyelins (SMs) compared to WDLPS [4]. Li et al., by comparing the lipid profiles with adjacent normal adipose tissues, discovered that glycolysis, purine metabolism, pyrimidine metabolism and phospholipid formation were up-regulated in both dedifferentiated and well-differentiated retroperitoneal liposarcoma tissues, while tricarboxylic acid cycle, lipid absorption synthesis, fatty acid degradation and biosynthesis, as well as glycine, serine, and threonine metabolism were down-regulated in both DDLPS and WDLPS tissues compared with adjacent normal adipose tissues [20]. In another study, Patt et al. conducted metabolomic and lipidomic analyses of patient-derived DDLPS cell lines. They identified 17 metabolites with varying abundances, including ceramides, glycosylated ceramides, and sphingomyelin, which differed between cell lines with higher and lower MDM2 amplification [21]. These findings suggest that alterations in lipid metabolism may render DDLPS cell lines with high MDM2 amplification more aggressive [21]. Further study is needed to elucidate the metabolic features and related prognostic biomarkers between DDLPS and WDLPS.

Abnormal lipid metabolism and lipid metabolic reprogramming are closely related to cell signal transduction, drug resistance, immune microenvironment adaptation and other processes; These factors are thought to play important roles in the occurrence and development of tumors [17–19]. Zhou et al. compared the lipid profiles of WDLPS and DDLPS using the LC-MS/MS method. They found that WDLPS contains a large numbers of neutral lipid components, such as triglycerides and diacylglycerols, whereas DDLPS is composed of more phospholipids, such as phosphocholines (PCs), phosphoethanolamines (PEs), and sphingomyelins (SMs) compared to WDLPS [4]. Li et al., by comparing the lipid profiles with adjacent normal adipose tissues, discovered that glycolysis, purine metabolism, pyrimidine metabolism and phospholipid formation were up-regulated in both dedifferentiated and well-differentiated retroperitoneal liposarcoma tissues, while tricarboxylic acid cycle, lipid absorption synthesis,

fatty acid degradation and biosynthesis, as well as glycine, serine, and threonine metabolism were down-regulated in both DDLPS and WDLPS tissues compared with adjacent normal adipose tissues [20]. In another study, Patt et al. conducted metabolomic and lipidomic analyses of patient-derived DDLPS cell lines. They identified 17 metabolites with varying abundances, including ceramides, glycosylated ceramides, and sphingomyelin, which differed between cell lines with higher and lower MDM2 amplification [21]. These findings suggest that alterations in lipid metabolism may render DDLPS cell lines with high MDM2 amplification more aggressive [21]. Further study is needed to elucidate the metabolic features and related prognostic biomarkers between DDLPS and WDLPS.

Therefore, identifying the metabolic features, genomic characteristics, distinctive molecular and signaling pathways that distinguish WDLPS from DDLPS is important for developing druggable targets, identifying biomarkers to predict prognosis, and improving patient outcomes. Based on the adipocyte origin of liposarcoma, a comprehensive analysis of lipid metabolism combined with transcriptomic characteristics can help identify valuable biomarkers. Therefore, in this study, we performed integrated lipidomic and RNA sequencing analyses of tissues from patients with retroperitoneal WDLPS and DDLPS.

Materials and methods

Patients and samples

In total, 48 tumor samples (19 WDLPS and 29 DDLPS) and 128 blood samples (35 WDLPS and 93 DDLPS) were obtained from 128 patients diagnosed with retroperitoneal liposarcoma (RLPS) who underwent surgery between 2015 and 2021 at Peking University Cancer Hospital. A total of 48 samples were analyzed for RNA-seq and 20 of these were also analyzed for lipidomics and combined analysis. We excluded patients with other known active malignant tumors and those who received any form of antitumor treatment, including chemotherapy, radiotherapy, targeted therapy, or immunotherapy prior to surgery. Pathology confirmation of RLPS was independently reviewed by two experienced pathologists in the Department of Pathology. Serum was collected from patients before surgery and stored at −80 °C for subsequent enzyme-linked immunosorbent assay (ELISA). The study was approved by the Medical Ethics Committee of Peking University Cancer Hospital (2022KT84). Written informed consent was obtained from all participants. Detailed clinicopathological information is listed in Table 1.

Table 1 Clinical characteristics of 128 patients with WDLPS or DDLPS

Characteristics	WDLPS (*n* = 35)	DDLPS (*n* = 93)
Age (y)	54.5 ±9.3	55 ±11.0
Gender, *n* (%)		
Male	13 (37.1)	55 (59.1)
Female	22 (62.9)	38 (40.9)
Presentation *n* (%)		
Primary	25 (71.4)	49 (52.7)
Recurrent	10 (28.6)	44 (47.3)
Tumor size (cm)	24.3 ±9.3	21.8 ±9.3
Surgical margin, *n* (%)		
R0/R1	33 (94.3)	85 (91.4)
R2	2 (5.7)	8 (8.6)
FNCLCC grade		
G1	35 (100)	0 (0)
G2	0 (0)	48 (51.6)
G3	0 (0)	45 (48.4)

Lipid extraction

Lipid was extracted from a 50-mg solid sample using a multistep procedure. Briefly, liposarcoma samples were homogenized at −10 °C using a high-throughput tissue crusher operating at 55 Hz for 10 min and then sonicated at 40 kHz for 28 min at 4 °C. Subsequently, samples were placed at −25 °C for 25–30 min and then centrifuged at 13,000 × *g* at 4 °C for 15 min. Centrifugation resulted in two-phase layers, and the cleared supernatants were carefully transferred to another tube and evaporated to dryness. For UHPLC-MS/MS analysis, the desiccated samples were reconstituted in a 120 µL loading solution consisting of isopropanol and acetonitrile (1:1) through a short sonication process in a 4 °C water bath. The extracted lipids were centrifuged for 20 min at 13,000 × *g* at 4 °C, after which the clear supernatant was transferred. Lastly, 2–3 µL portions of each prepared sample were injected into the UHPLC-MS/MS system.

UHPL-CMS/MS analysis

UHPLC-MS/MS analysis was performed using the UHPLC-Q Exactive HF-X Vanquish Horizon system (Thermo, USA) with an Accucore C30 column (100 mm × 2.1 mm i.d., 2.6 µm). The mobile phases consisted of 10 mM ammonium acetate in ACN and H2O (1:1) (as solvent A), while solvent B contained 2 mM ammonium acetate in a combination of ACN, IPA, and H2O (10:88:2). The typical parameters were as follows: 2 µL injection volume, 0.4 mL/min flow rate, 40 °C column temperature, and a total chromatographic separation time of 25 min. The solvent gradient used the following parameters: a gradual increase from 35 to 60% B over 0–5 min; a subsequent increase from 61 to 85% B over 5–13 min; from 86 to 100% B over 13–16 min; holding at 100% B for 17–19 min; from 100 to 35% B over 19–20 min; holding at 35% B until separation was complete. All samples were kept at 4 °C during the analysis. Data were collected using the UHPLC-Q Exactive HF-X Benchtop Orbitrap

Mass Spectrometer (Thermo) equipped with an HESI and operated in positive and negative ion modes. Data collection was performed using the Data Dependent Acquisition method across a mass spectrum of 200 to 2000 m/z. After UHPLC-MS/MS analyses, the raw data were imported into LipidSearch software (Thermo, CA) for peak detection, alignment, and identification. Lipid identification was based on MS/MS fragmentation, and the data were analyzed using the Majorbio online platform (cloud.majorbio.com).

Differentially abundant metabolite analysis

The R package was employed for conducting PCA and OPLS-DA analysis. Metabolites showing significant differences were selected based on the Variable Importance in the Projection (VIP) derived from the OPLS-DA model and the *P*-value of the Student's *t*-test. Metabolites with VIP > 1 and $P < 0.05$ were considered statistically significant.

RNA-sequencing analysis

Liposarcoma tissues obtained during surgical treatment were subjected to total tissue RNA extraction using TRIzol Reagent (Invitrogen). The extracted RNA was assessed and quantified, and only samples met stringent quality criteria, including OD260/280 = 1.8 to 2.2, OD 260/230 ≥ 2.0, RIN ≥ 6.5, 28 S:18 S ≥ 1.0, and mass > 2.0 μg. Total RNA purification, reverse transcription, construction libraries, and sequencing were all conducted at Shanghai Majorbio Bio-pharm Biotechnology following the Illumina instructions (San Diego, CA). After quantification, the paired-end RNA-seq library underwent sequencing on an Illumina NovaSeq 6000 sequencer with a read length of 2×150 bp. SeqPrep (https://github.com/jstjohn/SeqPrep) default parameters were employed for trimming and quality control of raw paired-end reads. Subsequently, the clean reads were aligned individually to the reference genome in orientation mode using TopHat (http://tophat.cbcb.umd.edu/). The raw RNA-seq data have been deposited in the NCBI Sequence Read Archive (SRA) database under the BioProject ID: PRJNA1053633.

Differential expression analysis and functional enrichment

Transcript levels were quantified as transcripts per million reads (TPM) to identify differentially expressed genes (DEGs) between two distinct tumor samples. Gene abundances were determined using RSEM (http://deweylab.biostat.wisc.edu/rsem/), and DESeq2 was employed for differential expression analysis. Genes meeting the criteria of $|\log2FC| \geq 1$ and FDR < 0.05 (DESeq2) were considered as significant DEGs. GO functional enrichment, KEGG, and Reactome analyses were performed to identify significantly enriched DEGs, with significance determined by a Bonferroni-corrected $P < 0.05$ compared to the whole transcriptome. The RNA sequencing data were further compared with the secretory protein-encoding gene dataset from the Human Protein Atlas database (https://www.proteinatlas.org/).

Immunoblotting

For immunoblotting, liposarcoma tissue samples were homogenized, and the proteins from the tumor tissue were extracted. These proteins were then separated through SDS-PAGE electrophoresis and transferred from gels onto PVDF membranes. The membranes were subsequently incubated with various primary antibodies (anti-ECM1, anti-FN1, anti-MMP11, anti-TIMP1, and anti-GPNMB from ABclonal; anti-β-actin from ImmunoSci). Immunoblots were analyzed using a ChemiDoc XRS + instrument (Bio-Rad, USA).

Enzyme-linked immunosorbent assay (ELISA)

Commercially available human ECM1, FN, TIMP1, MMP11, and GPNMB sandwich ELISA kits (ImmunoSci, China) were used to assess serum protein levels in patients with WDLPS or DDLPS following the manufacturer's protocols. The absorbance of each well was measured at a wavelength of 450 nm using an enzyme microplate reader.

Immunohistochemical staining assay

Liposarcoma samples were fixed in 4% paraformaldehyde for 48 h and then embedded in paraffin. The tumor tissue sections were dried at 60 °C, deparaffinized using xylene, and washed with PBS for 20 min at room temperature. Subsequently, the tissue sections were microwaved in a sodium citrate buffer (1 mM, pH = 6) and then slowly cooled to reach room temperature. After quenching endogenous peroxidase activity with 3% H_2O_2, the tissue slides were blocked with 1% BSA for 40 min at 37 °C. The slides were then separately incubated with anti-ECM1, anti-FN1, anti-MMP11, anti-TIMP1, and anti-GPNMB antibodies (1:200) overnight at 4 °C, followed by incubation with a horseradish peroxidase-conjugated secondary antibody at 37 °C for 40 min. The color reaction was developed using 3,3′-diaminobenzidine (DAB) according to the kit protocols provided by ZSGB-BIO.

Histological analyses

Freshly obtained liposarcoma samples were fixed using 4% paraformaldehyde and subsequently embedded in paraffin after dehydration. The paraffin-embedded tumor tissues underwent hematoxylin/eosin (HE) staining for the identification of the tumor structure. Additionally, Sirius red and Masson's trichrome staining was performed to assess extracellular interstitial fibrosis. NDP.view2 imaging workstation was used to obtain images.

Statistical analysis

Data is presented as the mean ± standard error of the mean (SEM) and/or median (range) as suitable, except for lipidomics and RNA sequencing data. The Shapiro–Wilk test was initially performed for normality. For normally distributed data, the significance of group differences was assessed using an unpaired two-tailed Student's *t*-test for the comparison of the two groups. For non-normally distributed data, the Mann–Whitney *U* test was performed to compare two groups, whereas the Kruskal-Wallis H-test, followed by the Dunn-Bonferroni was performed to compare multiple groups. The Cox proportional hazard regression model was performed for univariate and multivariate analysis to identify independent prognostic factors that impact overall survival (OS) and recurrence-free survival (RFS). RFS is defined as the period starting from the surgical date until either the date of tumor recurrence or the most recent follow-up. OS is defined as the interval from the surgical date until either the date of death or the most recent follow-up. Each statistical experiment of Western-Blot was independently repeated three times. A *P*-value < 0.05 was considered statistically significant.

Results

Clinical characteristics of the patients

In total, 128 patients diagnosed with RLPS were included in this study, including 35 patients with WDLPS and 93 patients with DDLPS who underwent surgical treatment at Peking University Cancer Hospital. Tissue samples from 48 tumors (19 WDLPS and 29 DDLPS) and blood samples from all 128 patients (35 WDLPS and 93 DDLPS) were collected. The clinical characteristics of all 128 patients with RLPS are shown in Table 1. Among patients with WDLPS, 37.1% were male, and the mean age at diagnosis was 54.5 ± 9.3 years. In the DDLPS group, 59.1% of the patients were male, and the mean age at diagnosis was 55 ± 11.0 years. Primary tumors constituted 71.4% of the WDLPS cases, with a mean tumor size of 24.3 ± 9.3 cm, whereas 52.7% of the DDLPS cases were primary tumors, with a mean tumor size of 21.8 ± 9.3 cm. Among the 35 patients diagnosed with WDLPS who underwent surgery, 33 patients (94.3%) had successful gross complete resection (R0/R1), whereas 2 patients (5.7%) had residual disease (R2). Among the 93 patients with DDLPS who underwent surgery, 85 (91.4%) achieved gross complete resection (R0/R1), and 8 (8.6%) achieved residual disease (R2). Within the DDLPS group, 48 cases (51.6%) were classified as FNCLCC G2 and 45 cases (48.4%) were categorized as FNCLCC G3. Transcriptome analysis was performed on all 48 tumor samples, with 20 samples (9 WDLPS and 11 DDLPS) undergoing integrated lipidomic and transcriptomic analyses. The clinical characteristics of the 48 patients were obtained via transcriptomic analysis, and the 20 patients were obtained via lipidomic analysis (Supplementary Table S1 and Table S2).

Lipidomic analysis revealed lipid changes and enrichment pathways between WDLPS and DDLPS

Because retroperitoneal liposarcoma originates from adipose tissue, we determined the changes in lipid metabolism of WDLPS and DDLPS and the potential pathways related to the differentiation of liposarcoma. We performed high-throughput LC-MS/MS lipidomics studies on tumor samples from 9 patients diagnosed with WDLPS and 11 patients diagnosed with DDLPS. PCA visually showed clear intergroup separation of the lipidome score plots of the two groups (Fig. 1A). In total, 1621 metabolites were detected, revealing 618 significantly changed lipids between WDLPS and DDLPS. The volcano plot showed 339 upregulated lipids, and the most significant differences were found in phosphatidylcholines (PCs) and PEs. Furthermore, 279 lipids were downregulated, and triacylglycerides (TGs) were more notable in DDLPS than in WDLPS (fold change > 1 or <-1, VIP > 1, and $P < 0.05$) (Fig. 1B). A heatmap further verified the increase in PCs and PEs and the decrease in the abundance of specific TGs, such as TG (18:0/18:0/18:1), TG (20:2/18:2/18:2), TG (18:1/12:0/18:1) and TG (18:1/18:1/20:5), in DDLPS than in WDLPS (Figure S1A). Variable Importance of Projection (VIP) analysis of metabolites was subsequently performed using a cluster heatmap and a VIP bar chart to visualize the abundance patterns and associated *P*-values of the metabolites in both groups. Notably, compared with those in WDLPS, the increased metabolites exhibiting VIP > 2 in DDLPS were mainly composed of PC (18:0/22:4), PC (20:1/22:6), PC (24:2/20:4) and PC (18:1/22:1). However, the significantly downregulated metabolites with VIP > 2 were mainly TGs (Fig. 1C). Furthermore, KEGG enrichment analysis revealed lipid metabolic pathways, especially choline metabolism in cancer, glycerophospholipid metabolism, sphingolipid signaling pathway, adipocytokine signaling pathway, fat digestion and absorption, regulation of lipolysis in adipocytes, and sphingolipid metabolism (marked with red boxes), which were involved in most of the top 20 enrichment pathways ($P < 0.05$) (Fig. 1D). Altogether, these findings indicate substantial lipid changes and enrichment pathways that distinguish between WDLPS and DDLPS.

RNA sequencing analysis revealed that the DEGs were significantly enriched in lipid metabolism, development, and extracellular matrix pathways between WDLPS and DDLPS

We further investigated the whole transcriptomes of both WDLPS ($n = 19$) and DDLPS ($n = 29$) tumor samples using the Illumina RNA-Seq technology and found

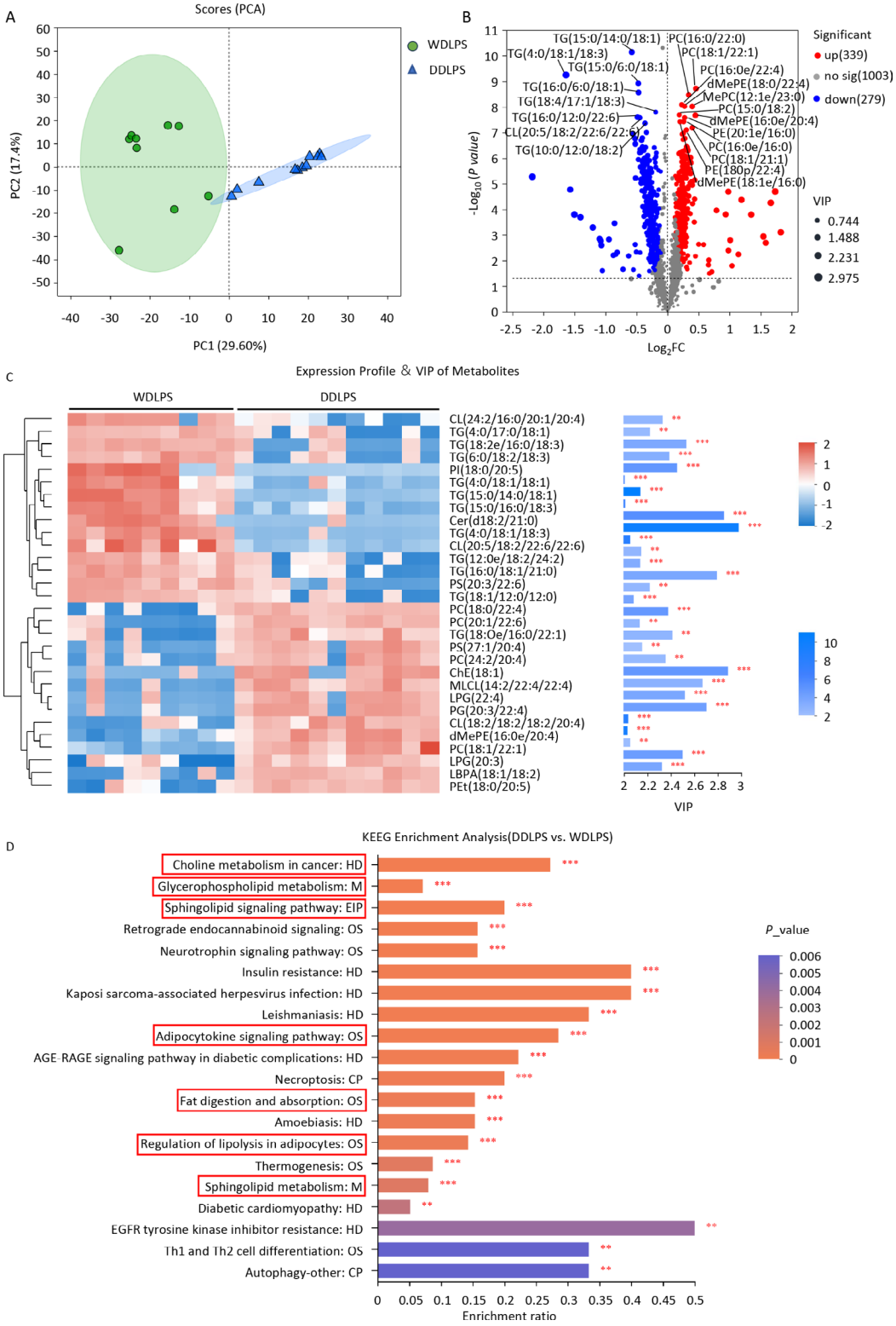

Fig. 1 Lipidomic analysis of DDLPS and WDLPS. (**A**) PCA score plot of DDLPS and WDLPS. Each green circle represents a WDLPS sample, and each blue triangle represents a DDLPS sample. (**B**) Volcano plot showing the number of significantly changed lipids between the two subtypes of tumors, and the top 20 altered lipids are labeled. (**C**) Expression Profile and VIP of metabolites between DDLPS and WDLPS; * $P<0.05$, ** $P<0.01$, and *** $P<0.001$. (**D**) The significantly changed lipids enriched in the KEGG pathway between WDLPS and DDLPS; ** $P<0.01$, and *** $P<0.001$; $n=9$ for the WDLPS group and $n=11$ for the DDLPS group

significant differences in gene expression profiles and potential signaling pathways between these distinct types of liposarcoma. Compared with the WDLPS group used as the control, we identified 1630 DEGs in the DDLPS group, among which 993 were upregulated, and 637 were downregulated (P-value < 0.05, $|\log_2 FC| \geq 1$) (Fig. 2A). The heatmap revealed the top 50 genes displaying significant differences between the two groups (Fig. 2B). Furthermore, Gene Ontology (GO) enrichment analysis of the DEGs showed enrichment in pathways associated with lipid metabolism (highlighted with red boxes), including response to fatty acid, fatty-acyl-CoA metabolic process, lipid storage, fatty acid derivative biosynthetic process, and fatty-acyl-CoA biosynthetic process. Pathways associated with development (marked with blue boxes), including chondrocyte development, regulation of biomineral tissue development, negative regulation of cellular response to growth factor, and biomineral tissue development, were significantly enriched among the top pathways (Fig. 2C and D). Further enrichment analysis, including KEGG and Reactome analyses, showed significant enrichment in lipid metabolic pathways (marked with red boxes) and extracellular matrix (ECM) pathways, including ECM-receptor interaction, ECM organization, and elastic fiber formation (highlighted with blue boxes) (Fig. 2E, S2A, S2B, S2C). Gene set enrichment analysis (GSEA) of the RNA-seq data revealed GO terms (NES > 1 or NES < −1 and P < 0.05), among which fatty acid beta-oxidation (GO:0006635) and fatty acid catabolic process (GO:0009062) were considerably enriched in gene sets positively correlated with WDLPS (Fig. 2F and G). However, collagen fibril organization (GO:0030199) was one of the top significantly enriched gene sets positively correlated with DDLPS (Fig. 2H).

Integrated lipidomic and transcriptomic analysis identified 29 genes as potential biomarkers between WDLPS and DDLPS

A comprehensive analysis was further performed, and Procrustes analysis showed a strong correlation between the lipidome and transcriptome. The values of M2 (0.643) and P(0.001) indicated significant congruence in the relationship between lipid metabolites and the transcriptional gene profile in both WDLPS and DDLPS (Fig. 3A). Furthermore, our investigation of the regulatory networks of genes and metabolites showed that the majority of DEGs were intricately associated with key lipid metabolites, such as Cer (t17:0/25:0), TG (16:1/16:1/18:1), and PC (26:1/16:0) (Fig. 3B). Through combined lipidomics and RNA-seq analysis, we identified 196 genes significantly correlated with 48 metabolites (Figure S3A). KEGG co-enrichment analysis showed significant associations (P < 0.05) with pathways, including cholesterol metabolism, fat digestion and absorption, regulation of lipolysis in adipocytes, calcium signaling pathway, and cAMP signaling pathway (Fig. 3C). In fact, although these 196 genes and 48 metabolites were not subsequently verified in this study, they are crucial for future metabolic and functional research in liposarcoma. KEGG enrichment analysis of 196 differential genes significantly enriched in lipid metabolism including Glyoxylate and dicarboxylate pathways, Glycerolipid metabolism, Valine leucine and isoleucine degradation, insulin signaling pathway, PPAR signaling pathway, Regulation of lipolysis in adipocytes, Fatty acid elongation, Butanoate metabolism, Fat digestion and absorption, Fatty acid degradation, pyruvate metabolism, Lysine degradation, beta-Alanine metabolism (Figure S3B). This integrated analysis, along with the results from our lipidomics, showed PCs and TGs as crucial differentiators between WDLPS and DDLPS. Furthermore, 73 genes were positively associated with PCs and negatively associated with TGs. Overlapping these genes with the 1630 DEGs identified in the transcriptome and the dataset of secretory protein-encoding genes from the Human Protein Atlas database (https://www.proteinatlas.org/) led to the identification of 29 genes as potential secretory serum biomarkers for differentiating liposarcoma at different degrees of differentiation (Fig. 3D and E). Furthermore, GO enrichment analysis of these 29 genes showed that the ECM and developmental process were involved in most of the top significantly enriched pathways (marked with red boxes) (Fig. 3F, S3C).

Validation of proteins and assessing the collective diagnostic efficacy of five biomarkers at the tumor tissue level

To further determine the expression of developmental-related and ECM-related genes at the protein level, tumor tissues were collected and evaluated by western blotting assay. This analysis confirmed significant differences in 5 proteins among the 29 genes. Compared with WDLPS, DDLPS showed increased levels of tissue inhibitors of metalloproteinases-1 (TIMP1), fibronectin 1 (FN1), matrix metallopeptidase 11 (MMP11), glycoprotein nonmetastatic melanoma protein B (GPNMB), and extracellular matrix protein 1 (ECM1) (Fig. 4A and B). Immunohistochemical staining also confirmed the changes in the levels of the aforementioned five proteins. The histological analysis of WDLPS mainly showed cells resembling mature adipocytes. On the other hand, DDLPS mainly included non-adipocytes (Fig. 4C). Additionally, Sirius red and Masson staining also showed that DDLPS exhibited more tissue collagen deposition than WDLPS, which is consistent with ECM pathway activation (Fig. 4C). GO enrichment analysis of these validated proteins showed their significant involvement in regulating developmental processes, with ECM1, FN1, TIMP1, and MMP11 prominently associated with ECM pathways

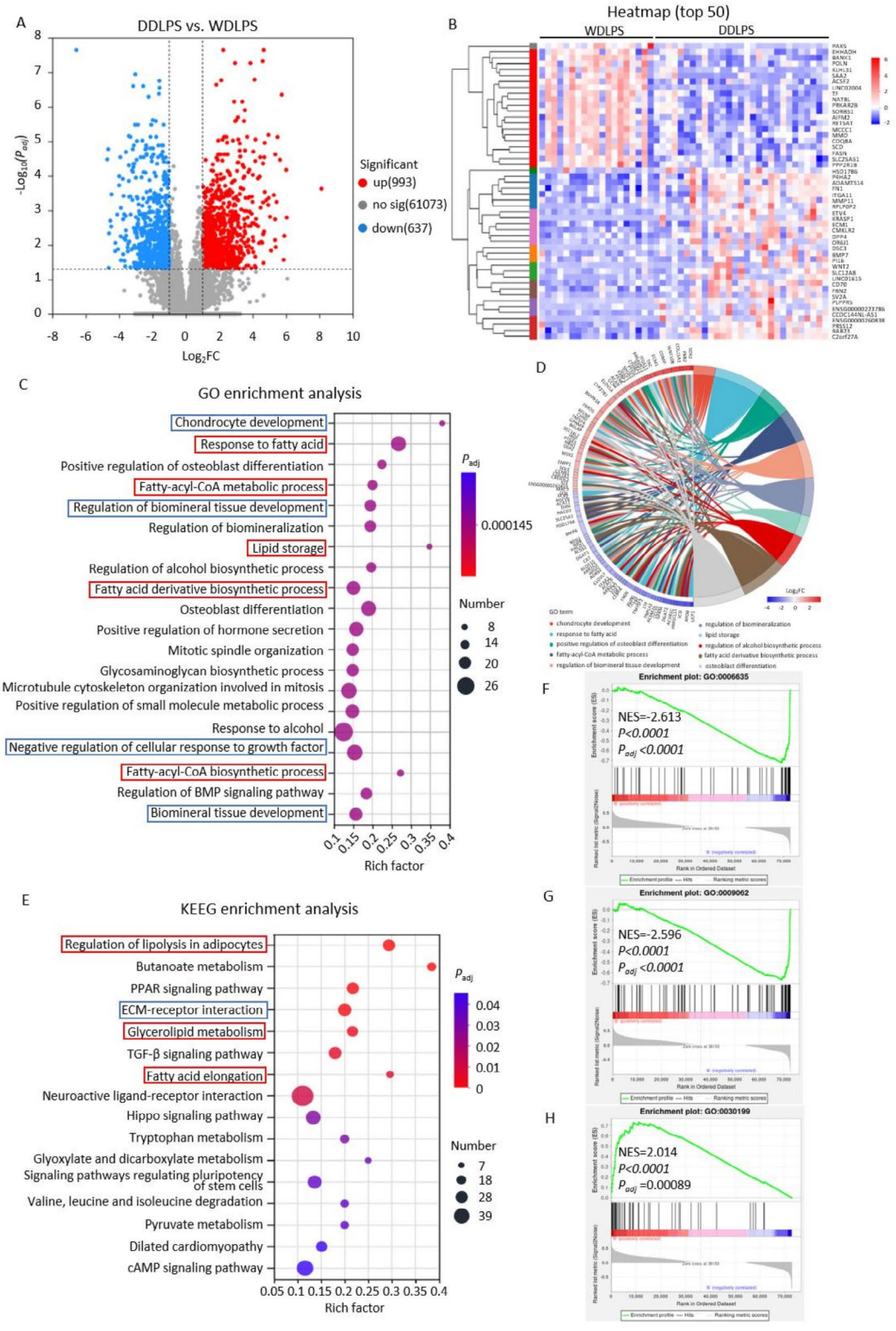

Fig. 2 RNA sequencing analysis between WDLPS and DDLPS. (**A**) Volcano plot showing the number of differentially expressed genes (DEGs) of WDLPS and DDLPS tissues; $P_{adj} < 0.05$, $n = 19$ for the WDLPS group and $n = 29$ for the DDLPS group. (**B**) A heatmap of the expression of the top 50 DEGs in the WDLPS and DDLPS groups. Red indicates high expression, and blue indicates low gene expression; $P_{adj} < 0.05$, $n = 19$ for the WDLPS group and $n = 29$ for the DDLPS group. (**C**) Gene Ontology (GO) functional enrichment analysis of the 1630 DEGs between WDLPS and DDLPS. (**D**) GO chord plot. (**E**) KEGG enrichment analysis of the 1630 DEGs between WDLPS and DDLPS. (**F**) Gene set enrichment analysis (GSEA) of fatty acid beta-oxidation (GO:0006635). (**G**) GSEA of the fatty acid catabolic process (GO:0009062). (**H**) GSEA of collagen fibril organization (GO:0030199)

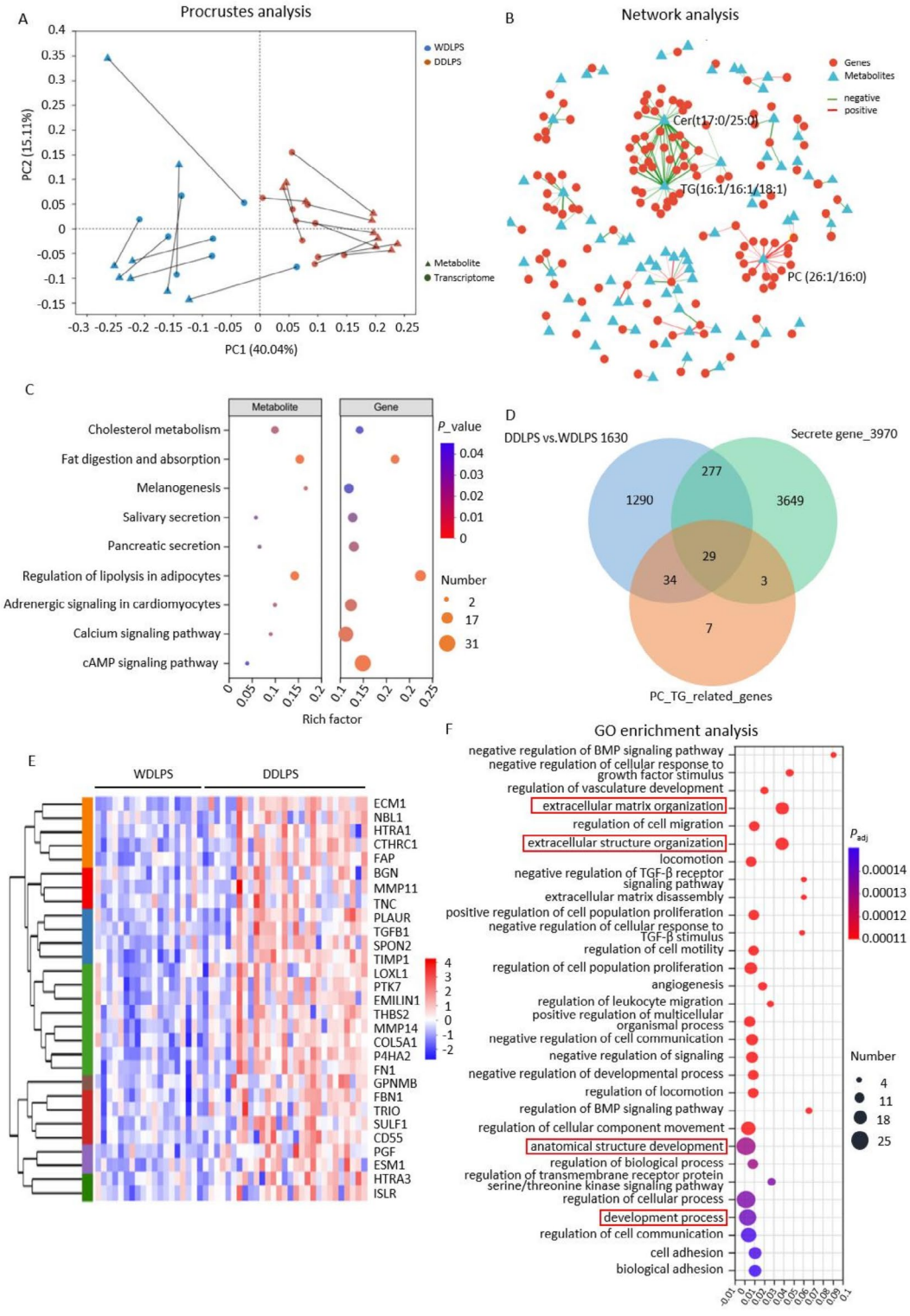

Fig. 3 Integrated lipidomic and transcriptomic analysis between WDLPS and DDLPS tissues. (**A**) Procrustes-transformed (PCA) score plots of metabolic and transcriptomic profiles between WDLPS and DDLPS. (**B**) Differential genes-to-differentially abundant metabolite network. (**C**) KEGG co-enrichment analysis between WDLPS and DDLPS. (**D**) A Venn diagram of 1630 DEGs (red), 73 genes positively linked to PCs and negatively linked to TGs (green), and 3970 secretory protein-encoding genes from the Human Protein Atlas database (blue) were intersected to obtain 29 DEGs. (**E**) A heatmap of the expression of the 29 DEGs between the WDLPS and DDLPS groups. (**F**) Gene Ontology (GO) functional enrichment analysis of the 29 DEGs between WDLPS and DDLPS

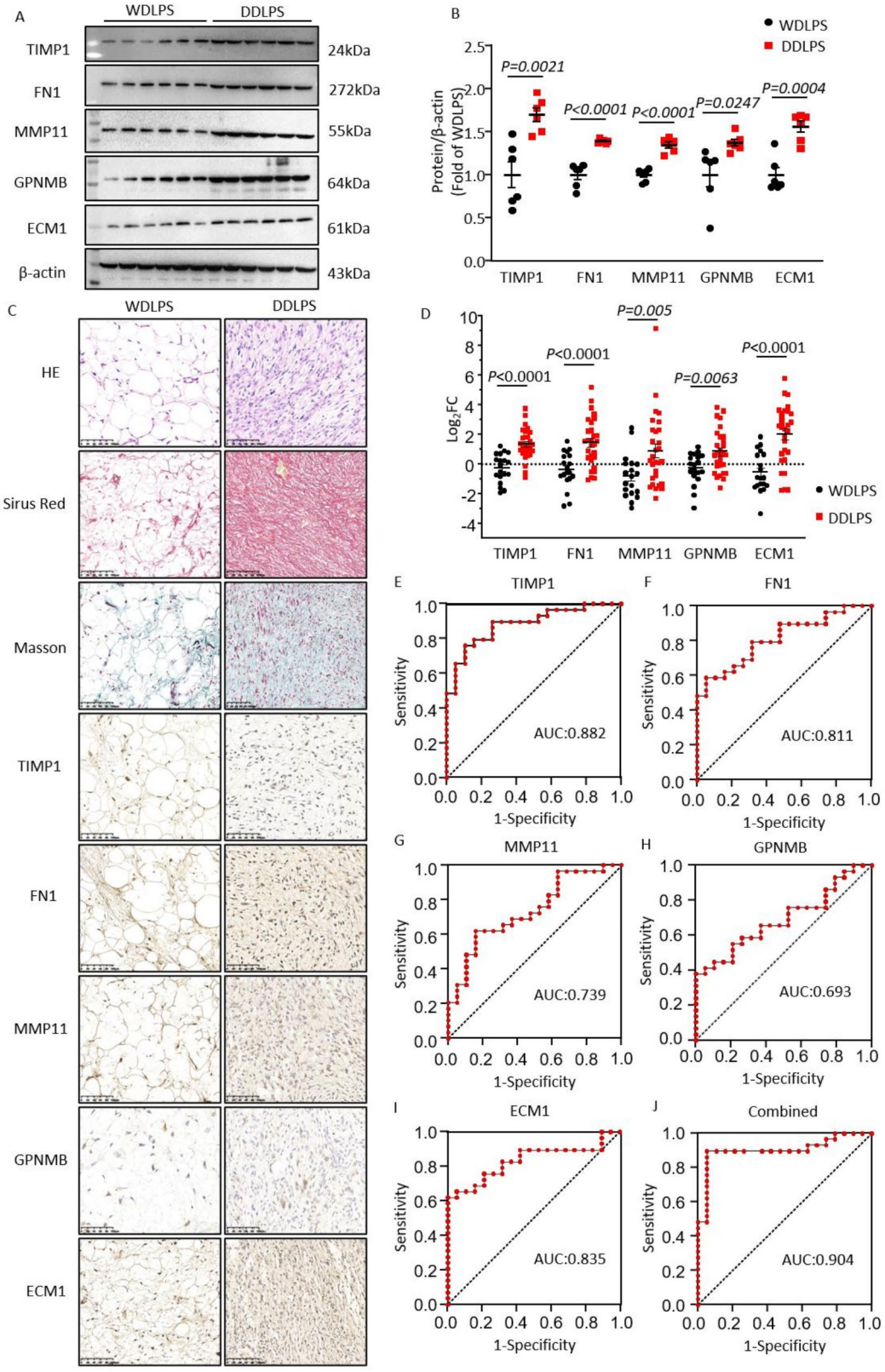

Fig. 4 (See legend on next page.)

(See figure on previous page.)

Fig. 4 Validation of proteins and assessment of the collective diagnostic efficacy of five biomarkers at the tumor tissue level (**A**) Western blot and average data (**B**) showing TIMP1, FN1, MMP11, GPNMB, and ECM1 protein levels in tumor tissues from WDLPS and DDLPS patients. $n=6$ for each group. (**C**) HE staining, picrosirius red, and Masson staining showing tumor morphology and collagen deposition in DDLPS and WDLPS tissues. Immunohistochemical staining of TIMP1, FN1, MMP11, GPNMB, and ECM1 in WDLPS and DDLPS tissues. Scale bar = 100 μm; $n=6$ for each group. (**D**) Statistical analysis of the five genes transcriptomic changes in WDLPS and DDLPS; $n=19$ for the WDLPS group and $n=29$ for the DDLPS group; $\log_2FC>0$ indicates that gene expression increased, and $\log_2FC<0$ indicates that gene expression decreased. (**E-J**) ROC curve of TIMP1, FN1, MMP11, GPNMB, ECM1, and the combination of five markers for WDLPS and DDLPS tumor tissues

(Figure S4A, S4B). Furthermore, a scatter plot was used to visually represent the individual $\log_2$ fold changes in the expression of these 5 genes between WDLPS and DDLPS tissues (Fig. 4D). Receiver operating characteristic (ROC) curves were constructed to show the specificity and sensitivity of both single-gene and five-gene combinations for diagnostic uses (Fig. 4E and J). When assessed individually, the area under the curve (AUC) for the five genes were as follows: 0.882 for TIMP1, 0.811 for FN1, 0.739 for MMP11, 0.693 for GPNMB, and 0.835 for ECM1. The optimal cutoff values for TIMP1, FN1, MMP11, GPNMB, and ECM1 for differentiating WDLPS from DDLPS were 652.1, 804.3, 8.4, 321.6, and 35.5, respectively. These values suggest sensitivities and specificities of 76% and 90% for TIMP1, 59% and 94% for FN1, 62% and 84% for MMP11, 38% and 100% for GPNMB, and 62% and 100% for ECM1, respectively (Fig. 4E and I). Furthermore, the combined evaluation of these genes exhibited a substantially higher AUC of 0.904, a sensitivity of 89.7%, and a specificity of 94.7% (Fig. 4J). These results indicate that these five differentially expressed genes hold potential as diagnostic markers for distinguishing between these distinct liposarcoma types.

Serum levels of ECM1 and GPNMB were significantly higher in DDLPS than in WDLPS, with ECM1 showing a gradual increase across varying FNCLCC grades

Based on the significance of detecting the serum protein concentration in the development of diagnostic biomarkers, we further used ELISA to detect changes in the aforementioned 5 proteins in the serum of 128 patients (Table 1). The median TIMP1, FN1, and MMP11 levels were similar between patients with WDLPS and patients with DDLPS (69.5 vs. 67.7 ng/mL, 103.8 vs. 101.4 ng/mL, 117.3 vs. 131.0 ng/mL, respectively), without statistically significant differences (Fig. 5A). The median GPNMB and ECM1 levels were significantly higher in patients with DDLPS than in patients with WDLPS (9.0 vs. 6.0 ng/mL, $P=0.0045$) (0.3262 vs. 0.1 891 ng/mL, $P<0.0001$) (Fig. 5A). ROC curves were generated to determine the optimal cutoff values to distinguish patients with WDLPS from patients with DDLPS. The optimal cutoff values for GPNMB and ECM1 in differentiating patients with DDLPS from patients with WDLPS were 9.1 ng/mL and 0.2836 ng/mL, respectively. These values confirmed a sensitivity and specificity of 48.4% and 82.9% for GPNMB, and 60.2% and 88.6% for ECM1, respectively. The combined evaluation of ECM1 and GPNMB showed a substantially higher AUC of 0.805, sensitivity of 75.3%, and specificity of 80% (Fig. 5B). The median GPNMB serum level was higher in G2 patients with DDLPS than in G1 patients with WDLPS, without statistically significant differences (7.9 vs. 6.0 ng/mL, $P=0.56$). Furthermore, the median GPNMB level was significantly higher in G3 patients with DDLPS than in G2 patients with DDLPS (10.3 vs. 7.9 ng/mL, $P=0.024$) and G1 patients with WDLPS (10.3 vs. 6.0 ng/mL, $P=0.001$) (Fig. 5C). The ECM1 level significantly increased from G1 WDLPS to G2 and G3 DDLPS, with median levels of 0.1891 (0.1585–0.249), 0.249 (0.1789–0.3751, $P=0.021$ vs. the G1 group) and 0.3709 (0.3051–0.7381, $P<0.001$ vs. the G1 group) ng/mL, respectively (Fig. 5C). These results indicate that the serum ECM1 and GPNMB levels in patients with DDLPS were significantly higher than those in patients with WDLPS, and ECM1 was gradually upregulated with increasing FNCLCC grade.

ECM1 and GPNMB serum levels negatively correlated with survival

Subsequently, a multivariate analysis was performed to identify the most crucial variables associated with OS and RFS. In total, 11 variables were selected for analysis, including age, gender, tumor size, presentation, surgical margin, FNCLCC stage, serum TIMP1 level, serum FN1 level, serum MMP1 level, serum GPNMB level, and serum ECM1 level. The median follow-up duration was 30.6 months (range, 14.8–52.2 months). Among the 128 patients, 52 died during the follow-up period, and 6 of 35 patients with WDLPS, 19 of 48 with G2 DDLPS, and 27 of 45 patients with G3 DDLPS died. In total, 43 of 118 patients underwent complete resection (R0+R1), and 9 of the 10 patients who underwent incomplete resection (R2) died. The only significant determinants of OS, according to the multivariate analysis, were malignancy grade ($P=0.023$), surgical margin ($P<0.001$), and serum GPNMB level ($P=0.019$) (Table 2). In the recurrence-free survival analysis, ten patients (2 WDLPS and 8 DDLPS) underwent incomplete resection (R2), leaving 118 patients for analysis. Recurrence occurred in 43 out of 118 patients (36.4%) after surgery at our institution. Among these, 5 out of 33 patients with WDLPS, 18 out of 46 with G2 DDLPS, and 20 out of 39 patients with G3 DDLPS developed recurrence. Additionally, 17 out of 71 primary patients and 26 out of 47 recurrent patients

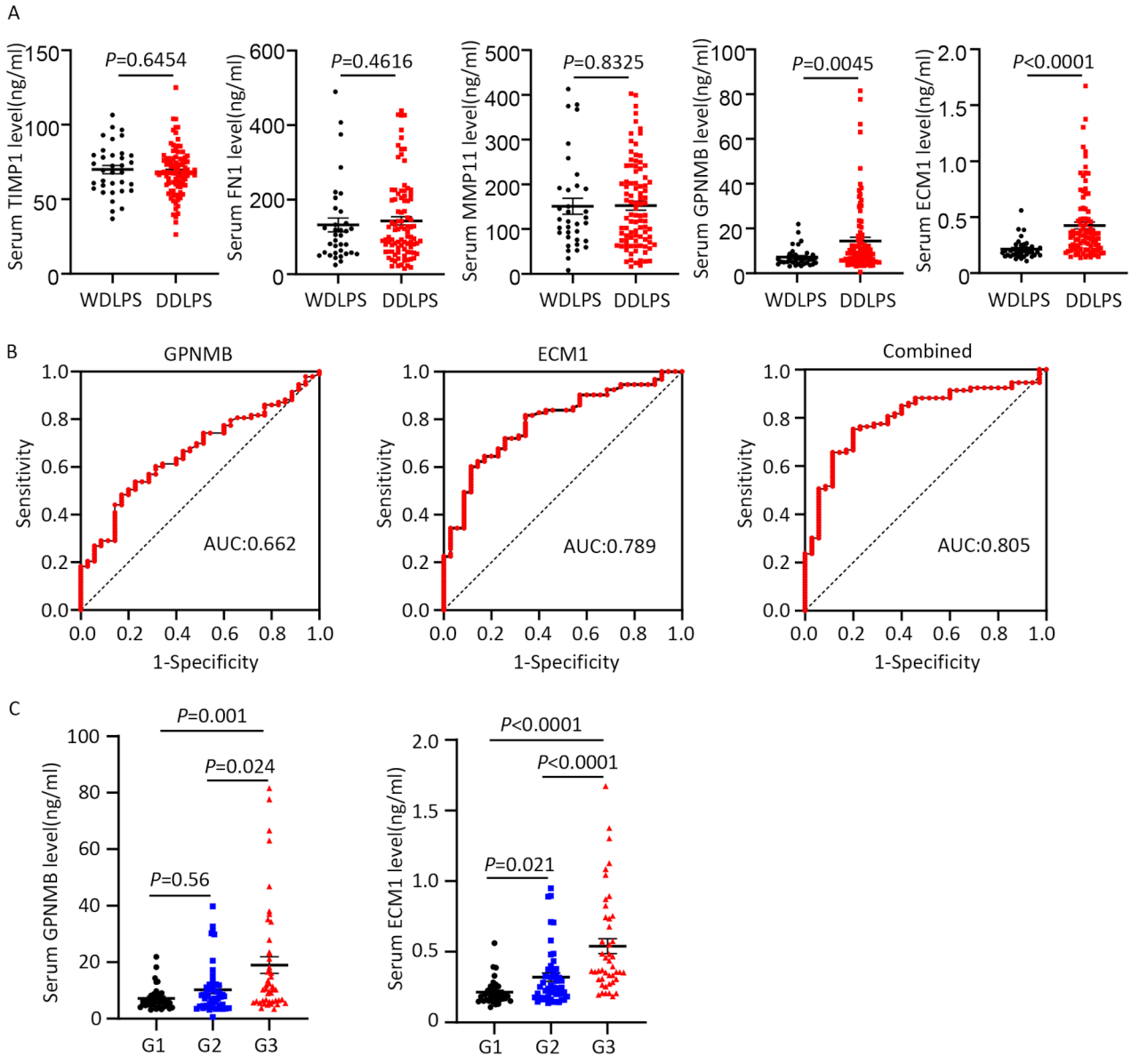

Fig. 5 The serum levels of ECM1 and GPNMB were significantly higher in DDLPS than in WDLPS, with ECM1 demonstrating a gradual increase across varying FNCLCC grades. (**A**) Serum protein levels of TIMP1, FN1, MMP11, GPNMB, and ECM1 in WDLPS and DDLPS patients. (**B**) ROC curve of the serum GPNMB, and ECM1 levels and the combination of the two biomarkers for patients with WDLPS or DDLPS. (**C**) Serum protein levels of GPNMB and ECM1 in the FNCLCC G1 WDLPS, G2, and G3 DDLPS. $n=35$ patients for the WDLPS group, and $n=93$ patients for the DDLPS group

experienced recurrence after surgery. The only significant determinants of RFS, according to the multivariate analysis, were malignancy grade ($P=0.027$), presentation (primary or recurrent) ($P=0.046$), and the serum ECM1 level ($P=0.043$) (Table 3). These results suggested a negative correlation between serum GPNMB levels and OS, and serum ECM1 levels and RFS.

Discussion

RLPS is a malignant tumor arising from mesenchymal tissue, exhibiting diverse levels of adipocytic differentiation [1]. Despite extensive research, the distinct genomic characteristics, biomarkers, metabolic features, and signaling pathways between WDLPS and DDLPS are unknown. In this study, we performed lipidomic analysis to compare DDLPS and WDLPS and observed significant lipid changes, notably an increase in phospholipids such as PCs and PEs, alongside a decrease in the metabolism of neutral lipids such as TGs. We found enriched lipid

Table 2 Results from the Cox Proportional Hazard models on OS

	Univariate Analysis			Multivariate Analysis		
	HR	**95%CI**	***P***	**HR**	**95%CI**	***P***
Patient's age (y)	1.019	0.991–1.049	0.181			
Sex			0.08			
Female vs. male	0.597	0.335–1.064				
Tumor size (cm)	1.018	0.990–1.047	0.209			
FNCLCC grade			< 0.001***			**0.023***
DD G2 vs. G1 WD	2.433	0.958–6.176		2.025	0.736–5.570	
DD G3 vs. G1 WD	5.518	2.268–13.424		3.897	1.393–10.903	
Presentation			0.022*			
Recurrent vs. Primary	1.928	1.101–3.376				
Surgical margin			< 0.001***			**< 0.001*****
R2 vs. R0 + R1	7.470	3.520–15.853		7.142	2.816–18.115	
FN1 (ng/mL)	1.001	0.999–1.003	0.341			
TIMP1 (ng/mL)	1.022	1.004–1.041	0.018*			
MMP11 (ng/mL)	0.996	0.993–1.000	0.036*			
GPNMB (ng/mL)	1.044	1.028–1.061	< 0.001***	1.027	1.004–1.050	**0.019***
ECM1 (ng/mL)	1.002	1.001–1.003	< 0.001***			

HR, hazard ratio; *P < 0.05; **P < 0.01; ***P < 0.001

Table 3 Results from the Cox Proportional hazards models on RFS

	Univariate Analysis			Multivariate Analysis		
	HR	**95%CI**	***P***	**HR**	**95%CI**	***P***
Patient's age (y)	1.005	0.976–1.035	0.741			
Sex			0.113			
Female vs. male	0.609	0.330–1.124				
Tumor size (cm)	1.014	0.980–1.048	0.433			
FNCLCC grade			0.001**			**0.027***
DD G2 vs. G1 WD	3.576	1.322–9.668		2.650	0.939–7.481	
DD G3 vs. G1 WD	6.181	2.303–16.586		4.361	1.479–12.858	
Presentation			0.001**			**0.046***
Recurrent vs. Primary	2.752	1.483–5.109		1.962	1.013–3.801	
FN1 (ng/mL)	1.000	0.998–1.003	0.752			
TIMP1 (ng/mL)	1.013	0.993–1.034	0.201			
MMP11 (ng/mL)	0.998	0.994–1.001	0.079			
GPNMB (ng/mL)	1.002	0.970–1.034	0.922			
ECM1 (ng/mL)	1.002	1.001–1.003	< 0.001***	1.001	1.000–1.003	**0.043***

HR, hazard ratio; *P < 0.05; **P < 0.01; ***P < 0.001

metabolic pathways distinguishing WDLPS from DDLPS. Furthermore, RNA sequencing analysis showed that the DEGs were significantly enriched in lipid metabolism, development, and ECM pathways between WDLPS and DDLPS. Integrated lipidomic and transcriptomic analysis revealed 29 genes that can be used as potential biomarkers for distinguishing WDLPS and DDLPS. Furthermore, we confirmed the changes in the protein levels of TIMP1, GPNMB, FN1, MMP11, and ECM1 in tumor tissues and evaluated the collective diagnostic efficacy of these five biomarkers. We performed ELISA to analyze serum samples from 128 patients and found markedly higher serum levels of ECM1 and GPNMB in patients with DDLPS than in patients with WDLPS. ECM1 exhibited a progressive increase across different FNCLCC grades and was negatively correlated with RFS. However, GPNMB levels showed a negative correlation with OS. These results have crucial translational significance for the development of RLPS serum markers.

Because sarcomas stem from adipocyte origins, determining lipid metabolism may clarify the differences between WDLPS and DDLPS. A previous study analyzed the metabolomic and lipidomic profiles of six patient-derived DDLPS cell lines and found 17 different metabolites, such as ceramides, glycosylated ceramides, and sphingomyelin, between patients with higher and lower MDM2 amplifications [21]. In an in vivo study, a liposarcoma mouse model with Notch activation specific to adipocytes identified abnormal pathways related to adipocyte differentiation [22, 23]. These studies helped

reveal the metabolic characteristics of liposarcomas. However, both in vitro and in vivo studies have some limitations. A recent study reported that the WDLPS predominantly contains many neutral lipids, such as TG and DG, whereas the lipids in the DDLPS contain a greater proportion of phospholipids, such as PCs, Pes, and SMs [4]. However, these findings, obtained from an analysis involving 6 patients with WDLPS and 7 patients with DDLPS, warrant further validation. Furthermore, the potential role of omics analysis in the early differential diagnosis and identification of prognostic biomarkers requires clarification. In this study, the lipidomic analysis revealed higher levels of phospholipids such as PCs and PEs and decreased metabolism of neutral lipids such as TGs in DDLPS than in WDLPS, which is consistent with the findings of previous research [4]. This suggests a greater phospholipid composition in DDLPS. Phospholipids are integral components of cellular membranes, playing crucial roles in chemical-energy storage, cell transformation, and cell–cell interactions, and contribute significantly to tumor cell progression and metastasis [24]. Hence, the distinct phospholipid compositions of the two liposarcoma subtypes might correlate with their differing malignant characteristics.

The previous studies have reported the genomic characteristics of both WDLPS and DDLPS. Notably, the amplification of Chr12q encodes important genes such as MDM2, CDK4, YEATS2, HMGA2, and CPM, mediating the development of both WDLPS and DDLPS [1, 2, 15, 16]. Furthermore, additional specific genomic changes, such as deletions at 11q23 and gains at 6q23 and 1p32, have been found as unique aberrations in DDLPS [2, 25]. Among the 1630 DEGs discovered in this study using transcriptomic analysis, we found increased levels of HMGA2 and HOXC13 and decreased levels of CPM, which is consistent with the results reported in previous studies [26–28]. Notably, our study revealed the downregulation of diacylglycerol O-acyltransferase 2 (DGAT2) in DDLPS, which is important for triacylglycerol biosynthesis and fat digestion and absorption [29]. Furthermore, the downregulated expression of G0/G1 switch gene 2 (G0S2), a regulator of lipid metabolism known to promote apoptosis by binding with BCL2 in DDLPS [30–32], was also verified through integrated exome and RNA sequencing from the Japan Sarcoma Genome Consortium [15]. The downregulation of DGAT2 and G0S2 expression likely contributes to the induction of dedifferentiation and malignant transformation in adipocytes. Pathway enrichment analysis revealed significant enrichment in lipid metabolic pathways, developmental pathways, and ECM pathways, as described in the results, and also in the peroxisome proliferator-activated receptor (PPAR) pathway. The PPAR pathway is recognized as a critical mediator of adipocyte differentiation in LPS [33], which was notably enriched. These findings provide novel insights into the metabolome and transcriptome characteristics of WDLPS and DDLPS.

Through combined integrated analysis, we identified 73 genes positively correlated with PCs and negatively correlated with TGs. We obtained 29 potential biomarkers by overlaying these 73 genes with the 1630 DEGs identified in the transcriptome and the secretory protein-encoding gene dataset from the Human Protein Atlas. These biomarkers were significantly enriched in developmental and ECM pathways. Western blotting and immunohistochemical staining confirmed significant increases in the protein levels of ECM1, FN1, TIMP1, MMP11, and GPNMB in DDLPS than in WDLPS. Moreover, based on the RNA sequencing results, a combined diagnosis using the five biomarkers yielded an AUC of 0.904. The ECM, composed of exocrine molecules, offers structural and biochemical support to the surrounding environment. A previous study showed that a changed ECM in adipose tissue is crucial for tumor development, by changing macromolecular components, degradation enzymes, and stiffness [34, 35]. TIMP1 was found to improve the growth and movement of DDLPS cells by activating YAP/TAZ, and the presence of high levels of TIMP1 in patients with DDLPS is associated with a negative prognosis [36]. GPNMB plays a role in adipogenesis, lipid metabolism, and immune regulation [37]. Another analysis of target antigens using RNA-seq data from the TCGA reported that GPNMB is highly expressed in the majority of sarcomas [38]. MMP-11 is highly expressed in osteosarcoma, and miR-125a-5p directly targets MMP-11 to inhibit cell migration, invasion, and EMT [35, 39]. FN1 was upregulated in chemo-resistant osteosarcoma cell lines and tissues [40] and affected cell communication, proliferation, and apoptosis in the 3D culture model of soft sarcoma [41]. ECM1 functions as a secreted factor to promote adipocyte differentiation and can also affect the energy metabolism of the entire body [42]. Moreover, ECM1 can facilitate cell metastasis and glucose metabolism by activating ITGB4/FAK/SOX2/HIF-1α signaling in gastric cancer [43].

Our survival analysis of postoperative patients indicates that high expression levels of ECM1 and GPNMB are associated with poor prognosis. This suggests that ECM1 and GPNMB may promote the development of malignant behavior of tumors. Previous studies have indicated that GPNMB, expressed on both melanoma cells and myeloid-derived suppressor cells (MDSCs), plays an immunosuppressive and tumor-promoting role in melanoma, making it a significant novel therapeutic target in these diseases. Glembatumumab vedotin, an antibody-drug conjugate (ADC) targeting GPNMB, has been evaluated in several early-phase clinical trials, particularly for melanoma and breast cancer. In breast cancer, it

shows the most promise in triple-negative breast cancer (TNBC) patients whose tumors express high levels of GPNMB. Further studies need to screen potential drugs and to examine ECM1 and GPNMB expression levels in both primary and recurrent liposarcoma patients to determine if there is a correlation between tumor progression and serum levels of these proteins. Our future research will further explore and publish functional validation of these finding through additional in vitro cell function and in vivo animal experiments.

Tumor biology and radical resection play crucial roles in the treatment of RLPS [44, 45]. Complete resection is the main potential cure for RLPS. However, due to the intricate anatomical confines within the retroperitoneum, achieving radical resection of tumors, which results in marginal excisions, is challenging [8, 46]. Although extended surgery can increase OS and RFS, potential risks associated with surgery and the occurrence of serious postoperative complications cannot be ruled out [8, 47, 48]. When extended surgery involves critical blood vessels or organs such as the inferior vena cava or pancreas, the surgical risks increase considerably [49]. Moreover, extended resection shows limited effect on OS and controlling local recurrence for patients with advanced stages or multiple recurrences [8, 50]. Therefore, understanding the distinct biological behaviors among various subtypes of sarcoma is important in establishing personalized treatment approaches [51]. Histological type, tumor grade, myogenic differentiation, osteogenic differentiation, and organ infiltration are crucial indicators of evaluating biological behavior [52–55]. However, they are difficult to obtain before surgery Although core needle biopsy and imaging techniques, such as CT, MRI, and PET-CT, can help reveal the biological behavior of liposarcoma, the results may be incomplete due to the great spatial heterogeneity within tumors [56–58]. Therefore, blood-based tumor markers serve as valuable supplements, facilitating a more accurate and comprehensive evaluation of the biological behavior of liposarcoma. Blood-based tests are readily accessible and inexpensive methods. For recurrent liposarcoma, the decision of surgery is challenging to make [46, 59]. Serum markers can act as predictors of malignant biological changes, monitoring the progression of dedifferentiated components, and serving as important reference points in deciding appropriate surgical intervention. Whether these serum markers can indicate the efficacy of drug therapies warrants further investigation through subsequent clinical studies.

Conclusions

To conclude, we performed integrated lipidomics and RNA sequencing analyses of tissues from patients with WDLPS and DDLPS. Lipidomics analysis revealed that PCs and PEs increased while TGs decreased significantly in DDLPS compared with WDLPS. RNA sequencing analysis revealed that significantly DEGs were enriched in lipid metabolism, developmental processes and extracellular matrix related biological processes. Integrated lipidomic and transcriptomic analysis identified 29 secreted protein coding genes as potential serum biomarkers between WDLPS and DDLPS. Western blot and immunohistochemical staining confirmed that the protein expression levels of TIMP1, FN1, MMP11, GPNMB and ECM1 in DDLPS tissues were significantly higher than those in WDLPS tissues. ELISA results showed that serum ECM1 and GPNMB levels in DDLPS patients were significantly higher than those in WDLPS group. The serum expression level of ECM1 was positively correlated with FNCLCC grade. Multivariate Cox regression analysis suggested that preoperative status (initial treatment or recurrence), surgical margin (R0/R1 or R2), FNCLCC grade, and serum GPNMB protein concentration were independent risk factors for postoperative OS in retroperitoneal liposarcoma. Preoperative status, FNCLCC grade and serum ECM1 protein concentration were independent risk factors for postoperative RFS in retroperitoneal liposarcoma. These findings provide an important foundation for the future diagnosis and prognosis prediction of patients with retroperitoneal liposarcoma having different differentiations.

Abbreviations

RLPS	Retroperitoneal Liposarcoma
LPS	Liposarcoma
WDLPS	Well-differentiated liposarcoma
DDLPS	Dedifferentiated liposarcoma
KEGG	Kyoto Encyclopedia of Genes and Genomes
GO	Gene Ontology
VIP	Variable Importance in the Projection
GESA	Gene set enrichment analysis
TCGA	The Cancer Genome Atlas
PCs	Phosphatidylcholines
PEs	Phosphoethanolamines
TGs	Triacylglycerides
TPM	Transcripts per million reads
DEGs	Differentially expressed genes
HE	Hematoxylin-eosin
ELISA	Enzyme linked immunosorbent assay
TIMP1	Tissue inhibitor of Metalloproteinases-1
FN1	Fibronectin 1
MMP11	Matrix Metallopeptidase 11
GPNMB	Glycoprotein Nonmetastatic Melanoma Protein B
ECM1	Extracellular Matrix Protein 1
OS	Overall Survival
RFS	Recurrence-free Survival
FNCLCC	Fédération Nationale des Centres de Lutte Contre le Cancer
ROC	Receiver Operating Characteristic
AUC	Area Under the Curve

Supplementary Information

The online version contains supplementary material available at https://doi.org/10.1186/s12935-024-03585-x.

Supplementary Material 1

Supplementary Material 2

Acknowledgements
We are grateful to Dr. Minghong Leng from Peking University Health Science Center and Tiancheng Chen for expert technical assistance.

Author contributions
C.H., X.W, J. Y. and H.Q. designed the project; X.W. and Q.L. collected tumor and blood samples from WDLPS and DDLPS patients; X.W., J.Y. and C.H. wrote the paper; J. Y. and W.J. performed the western-blot and ELISA experiments; Y. W. performed the immunohistochemical staining, and all the authors participated in the experimental design, data analysis, and data interpretation.

Funding
This study was supported by the Science Foundation of Peking University Cancer Hospital (XKFZ2421), Beijing Municipal Administration of Hospital's Ascent Plan (DFL20181104), Science Foundation of Peking University Cancer Hospital (2022-4), National Natural Science Foundation of China (82000348), Beijing Municipal Natural Science Foundation (7222193), Beijing Municipal Administration of Hospitals' Youth Programme (QML20181104), China Postdoctoral Science Foundation (2020M680260).

Data availability
All the data analyzed in the study are available from the published article and will be shared by corresponding author for reasonable request. The raw RNA-seq data were submitted to the NCBI Sequence Read Archive (SRA) database under the BioProject ID: PRJNA1053633.

Declarations

Ethics approval and consent to participate
The research protocol was conducted according to the guidelines of the Declaration of Helsinki and granted by the Medical Ethics Committee of Peking University Cancer Hospital (2022KT84). And all participants provided written informed consent.

Consent for publication
Not applicable.

Conflict of interest
None declared.

Author details
[1]Key Laboratory of Carcinogenesis and Translational Research (Ministry of Education/Beijing), Department of Hepato-Pancreato-Biliary Surgery, Peking University Cancer Hospital & Institute, Beijing 100142, P. R. China
[2]Trauma Treatment Center, Peking University People's Hospital; Key Laboratory of Trauma Treatment and Neural Regeneration (Peking University), National Center for Trauma Medicine, Beijing 100044, P. R. China
[3]Key Laboratory of Carcinogenesis and Translational Research (Ministry of Education/Beijing), Department of Pathology, Peking University Cancer Hospital & Institute, Beijing 100142, P. R. China
[4]Guowen (Changchun) International Hospital, Changchun 130000, P. R. China

Received: 1 February 2024 / Accepted: 26 November 2024
Published online: 18 December 2024

References

1. Lee ATJ, Thway K, Huang PH, Jones RL. Clinical and molecular spectrum of Liposarcoma. J Clin Oncol. 2018;36(2):151–9.
2. Tyler R, Wanigasooriya K, Taniere P, Almond M, Ford S, Desai A, Beggs A. A review of retroperitoneal liposarcoma genomics. Cancer Treat Rev. 2020;86:102013.
3. The WHO Classification of Tumours Editorial Board. WHO classification of Tumours Soft tissue and Bone Tumours. 5th ed. Lyon: IARC; 2020.
4. Song Z, Wang S, Lu L, Xu J, Zhou Q, Lu W, Tong H, Zhang Y, Liu W, Wang Z et al. Lipidomics and transcriptomics Differ Liposarcoma differentiation characteristics that can be altered by pentose phosphate pathway intervention. Metabolites 2022, 12(12).
5. Zhang J, Zhang L, Wang B, He L, Yu C, Peng Y, Xie M. Metastatic dedifferentiated liposarcoma invading the pulmonary vein and left atrium: a transesophageal echocardiographic insight. QJM. 2021;114(6):405–6.
6. Strauss DC, Hayes AJ, Thomas JM. Retroperitoneal tumours: review of management. Ann R Coll Surg Engl. 2011;93(4):275–80.
7. Kilpatrick SE. Dedifferentiated liposarcoma: a comprehensive historical review with proposed evidence-based guidelines regarding a diagnosis in need of further clarification. Adv Anat Pathol. 2021;28(6):426–38.
8. Deng H, Cao B, Cui H, Chen R, Li H, Zhao R, Chen L, Wei B. Clinical analysis of 5-year survival and recurrence in giant retroperitoneal liposarcoma after surgery. Chin Med J (Engl). 2023;136(3):373–5.
9. Lu J, Wood D, Ingley E, Koks S, Wong D. Update on genomic and molecular landscapes of well-differentiated liposarcoma and dedifferentiated liposarcoma. Mol Biol Rep. 2021;48(4):3637–47.
10. Callegaro D, Raut CP, Ajayi T, Strauss D, Bonvalot S, Ng D, Stoeckle E, Fairweather M, Rutkowski P, van Houdt WJ, et al. Preoperative radiotherapy in patients with primary retroperitoneal sarcoma: EORTC-62092 trial (STRASS) Versus off-trial (STREXIT) results. Ann Surg. 2023;278(1):127–34.
11. Vasella M, Gousopoulos E, Guidi M, Storti G, Song SY, Grieb G, Pauli C, Lindenblatt N, Giovanoli P, Kim BS. Targeted therapies and checkpoint inhibitors in sarcoma. QJM. 2022;115(12):793–805.
12. Blay JY, Chevret S, Le Cesne A, Brahmi M, Penel N, Cousin S, Bertucci F, Bompas E, Ryckewaert T, Soibinet P, et al. Pembrolizumab in patients with rare and ultra-rare sarcomas (AcSe Pembrolizumab): analysis of a subgroup from a non-randomised, open-label, phase 2, basket trial. Lancet Oncol. 2023;24(8):892–902.
13. Ingham M, Lee S, Van Tine BA, Choy E, Oza J, Doshi S, Ge L, Oppelt P, Cote G, Corgiat B, et al. A single-arm phase II trial of Sitravatinib in Advanced Well-Differentiated/Dedifferentiated Liposarcoma. Clin Cancer Res. 2023;29(6):1031–9.
14. Nassif EF, Cope B, Traweek R, Witt RG, Erstad DJ, Scally CP, Thirasastr P, Zarzour MA, Ludwig J, Benjamin R, et al. Real-world use of palbociclib monotherapy in retroperitoneal liposarcomas at a large volume sarcoma center. Int J Cancer. 2022;150(12):2012–24.
15. Hirata M, Asano N, Katayama K, Yoshida A, Tsuda Y, Sekimizu M, Mitani S, Kobayashi E, Komiyama M, Fujimoto H, et al. Integrated exome and RNA sequencing of dedifferentiated liposarcoma. Nat Commun. 2019;10(1):5683.
16. Louis-Brennetot C, Coindre JM, Ferreira C, Perot G, Terrier P, Aurias A. The CDKN2A/CDKN2B/CDK4/CCND1 pathway is pivotal in well-differentiated and dedifferentiated liposarcoma oncogenesis: an analysis of 104 tumors. Genes Chromosomes Cancer. 2011;50(11):896–907.
17. Grunt TW. Interacting Cancer machineries: Cell Signaling, lipid metabolism, and Epigenetics. Trends Endocrinol Metab. 2018;29(2):86–98.
18. Yu W, Lei Q, Yang L, Qin G, Liu S, Wang D, Ping Y, Zhang Y. Contradictory roles of lipid metabolism in immune response within the tumor microenvironment. J Hematol Oncol. 2021;14(1):187.
19. Martin-Perez M, Urdiroz-Urricelqui U, Bigas C, Benitah SA. The role of lipids in cancer progression and metastasis. Cell Metab. 2022;34(11):1675–99.
20. Xie F, Niu Y, Lian L, Wang Y, Zhuang A, Yan G, Ren Y, Chen X, Xiao M, Li X et al. Multi-omics joint analysis revealed the metabolic profile of retroperitoneal liposarcoma. Front Med 2023.
21. Patt A, Demoret B, Stets C, Bill KL, Smith P, Vijay A, Patterson A, Hays J, Hoang M, Chen JL et al. MDM2-Dependent rewiring of Metabolomic and Lipidomic profiles in Dedifferentiated Liposarcoma Models. Cancers (Basel) 2020, 12(8).
22. Bi P, Yue F, Karki A, Castro B, Wirbisky SE, Wang C, Durkes A, Elzey BD, Andrisani OM, Bidwell CA, et al. Notch activation drives adipocyte dedifferentiation and tumorigenic transformation in mice. J Exp Med. 2016;213(10):2019–37.
23. Tien PC, Chen X, Elzey BD, Pollock RE, Kuang S. Notch signaling regulates a metabolic switch through inhibiting PGC-1alpha and mitochondrial biogenesis in dedifferentiated liposarcoma. Oncogene. 2023;42(34):2521–35.
24. Bandu R, Mok HJ, Kim KP. Phospholipids as cancer biomarkers: Mass spectrometry-based analysis. Mass Spectrom Rev. 2018;37(2):107–38.
25. Mariani O, Brennetot C, Coindre JM, Gruel N, Ganem C, Delattre O, Stern MH, Aurias A. JUN oncogene amplification and overexpression block adipocytic differentiation in highly aggressive sarcomas. Cancer Cell. 2007;11(4):361–74.
26. Pentimalli F, Dentice M, Fedele M, Pierantoni GM, Cito L, Pallante P, Santoro M, Viglietto G, Cin PD, Fusco A. Retraction: suppression of HMGA2 protein

synthesis could be a Tool for the therapy of well differentiated Liposarcomas Overexpressing HMGA2. Cancer Res. 2018;78(24):6909.
27. Cantile M, Galletta F, Franco R, Aquino G, Scognamiglio G, Marra L, Cerrone M, Malzone G, Manna A, Apice G, et al. Hyperexpression of HOXC13, located in the 12q13 chromosomal region, in well–differentiated and dedifferentiated human liposarcomas. Oncol Rep. 2013;30(6):2579–86.
28. Klingbeil KD, Tang JP, Graham DS, Lofftus SY, Jaiswal AK, Lin TL, Frias C, Chen LY, Nakasaki M, Dry SM et al. IGF2BP3 as a Prognostic Biomarker in Well-Differentiated/Dedifferentiated Liposarcoma. *Cancers (Basel)* 2023, 15(18).
29. Liu Q, Siloto RM, Lehner R, Stone SJ, Weselake RJ. Acyl-CoA:diacylglycerol acyltransferase: molecular biology, biochemistry and biotechnology. Prog Lipid Res. 2012;51(4):350–77.
30. Heckmann BL, Zhang X, Xie X, Liu J. The G0/G1 switch gene 2 (G0S2): regulating metabolism and beyond. Biochim Biophys Acta. 2013;1831(2):276–81.
31. Welch C, Santra MK, El-Assaad W, Zhu X, Huber WE, Keys RA, Teodoro JG, Green MR. Identification of a protein, G0S2, that lacks Bcl-2 homology domains and interacts with and antagonizes Bcl-2. Cancer Res. 2009;69(17):6782–9.
32. Yang X, Lu X, Lombes M, Rha GB, Chi YI, Guerin TM, Smart EJ, Liu J. The G(0)/G(1) switch gene 2 regulates adipose lipolysis through association with adipose triglyceride lipase. Cell Metab. 2010;11(3):194–205.
33. Cristancho AG, Lazar MA. Forming functional fat: a growing understanding of adipocyte differentiation. Nat Rev Mol Cell Biol. 2011;12(11):722–34.
34. Yuan Z, Li Y, Zhang S, Wang X, Dou H, Yu X, Zhang Z, Yang S, Xiao M. Extracellular matrix remodeling in tumor progression and immune escape: from mechanisms to treatments. Mol Cancer. 2023;22(1):48.
35. Li J, Xu R. Obesity-Associated ECM remodeling in Cancer Progression. Cancers (Basel) 2022, 14(22).
36. Shrestha M, Ando T, Chea C, Sakamoto S, Nishisaka T, Ogawa I, Miyauchi M, Takata T. The transition of tissue inhibitor of metalloproteinases from − 4 to -1 induces aggressive behavior and poor patient survival in dedifferentiated liposarcoma via YAP/TAZ activation. Carcinogenesis. 2019;40(10):1288–97.
37. Gong XM, Li YF, Luo J, Wang JQ, Wei J, Wang JQ, Xiao T, Xie C, Hong J, Ning G, et al. Gpnmb secreted from liver promotes lipogenesis in white adipose tissue and aggravates obesity and insulin resistance. Nat Metab. 2019;1(5):570–83.
38. Pestana RC, Roszik J, Groisberg R, Sen S, Van Tine BA, Conley AP, Subbiah V. Discovery of targeted expression data for novel antibody-based and chimeric antigen receptor-based therapeutics in soft tissue sarcomas using RNA-sequencing: clinical implications. Curr Probl Cancer. 2021;45(5):100794.
39. Waresijiang N, Sun J, Abuduaini R, Jiang T, Zhou W, Yuan H. The downregulation of miR–125a–5p functions as a tumor suppressor by directly targeting MMP–11 in osteosarcoma. Mol Med Rep. 2016;13(6):4859–64.
40. Kun-Peng Z, Chun-Lin Z, Xiao-Long M, Lei Z. Fibronectin-1 modulated by the long noncoding RNA OIP5-AS1/miR-200b-3p axis contributes to doxorubicin resistance of osteosarcoma cells. J Cell Physiol. 2019;234(5):6927–39.
41. Bai C, Yang M, Fan Z, Li S, Gao T, Fang Z. Associations of chemo- and radioresistant phenotypes with the gap junction, adhesion and extracellular matrix in a three-dimensional culture model of soft sarcoma. J Exp Clin Cancer Res. 2015;34(1):58.
42. Challa TD, Straub LG, Balaz M, Kiehlmann E, Donze O, Rudofsky G, Ukropec J, Ukropcova B, Wolfrum C. Regulation of De Novo Adipocyte differentiation through Cross Talk between adipocytes and preadipocytes. Diabetes. 2015;64(12):4075–87.
43. Gan L, Meng J, Xu M, Liu M, Qi Y, Tan C, Wang Y, Zhang P, Weng W, Sheng W, et al. Extracellular matrix protein 1 promotes cell metastasis and glucose metabolism by inducing integrin beta4/FAK/SOX2/HIF-1alpha signaling pathway in gastric cancer. Oncogene. 2018;37(6):744–55.
44. Garcia-Ortega DY, Villa-Zepeda O, Martinez-Said H, Cuellar-Hubbe M, Luna-Ortiz K. Oncology outcomes in retroperitoneal sarcomas: prognostic factors in a Retrospective Cohort study. Int J Surg. 2016;32:45–9.
45. Tan MC, Brennan MF, Kuk D, Agaram NP, Antonescu CR, Qin LX, Moraco N, Crago AM, Singer S. Histology-based classification predicts pattern of recurrence and improves risk stratification in primary Retroperitoneal Sarcoma. Ann Surg. 2016;263(3):593–600.
46. Nathenson MJ, Barysauskas CM, Nathenson RA, Regine WF, Hanna N, Sausville E. Surgical resection for recurrent retroperitoneal leiomyosarcoma and liposarcoma. World J Surg Oncol. 2018;16(1):203.
47. Smith HG, Thomas JM, Smith MJ, Hayes AJ, Strauss DC. Multivisceral resection of retroperitoneal sarcomas in the elderly. Eur J Cancer. 2016;69:119–26.
48. Spolverato G, Chiminazzo V, Lorenzoni G, Fiore M, Radaelli S, Sanfilippo R, Sangalli C, Barisella M, Callegaro D, Gronchi A. Oncological outcomes after major vascular resections for primary retroperitoneal liposarcoma. Eur J Surg Oncol. 2021;47(12):3004–10.
49. Li CP, Wang Z, Liu BN, Lv A, Liu DN, Wu JH, Qiu H, Hao CY. Pancreaticoduodenectomy for retroperitoneal sarcomas: a Mono-Institutional experience in China. Front Oncol. 2020;10:548789.
50. Bonvalot S, Miceli R, Berselli M, Causeret S, Colombo C, Mariani L, Bouzaiene H, Le Pechoux C, Casali PG, Le Cesne A, et al. Aggressive surgery in retroperitoneal soft tissue sarcoma carried out at high-volume centers is safe and is associated with improved local control. Ann Surg Oncol. 2010;17(6):1507–14.
51. Dingley B, Fiore M, Gronchi A. Personalizing surgical margins in retroperitoneal sarcomas: an update. Expert Rev Anticancer Ther. 2019;19(7):613–31.
52. Kurzawa P, Mullen JT, Chen YL, Johnstone SE, Deshpande V, Chebib I, Nielsen GP. Prognostic value of myogenic differentiation in Dedifferentiated Liposarcoma. Am J Surg Pathol. 2020;44(6):799–804.
53. Gronchi A, Collini P, Miceli R, Valeri B, Renne SL, Dagrada G, Fiore M, Sanfilippo R, Barisella M, Colombo C, et al. Myogenic differentiation and histologic grading are major prognostic determinants in retroperitoneal liposarcoma. Am J Surg Pathol. 2015;39(3):383–93.
54. Yamashita K, Kohashi K, Yamada Y, Ishii T, Nishida Y, Urakawa H, Ito I, Takahashi M, Inoue T, Ito M, et al. Osteogenic differentiation in dedifferentiated liposarcoma: a study of 36 cases in comparison to the cases without ossification. Histopathology. 2018;72(5):729–38.
55. Zhao S, Zhao Y, Liu S, Zhang C, Wang X. Conditional survival after surgical resection of primary retroperitoneal tumors: a population-based study. Cancer Cell Int. 2021;21(1):60.
56. Thavikulwat AC, Wu JS, Chen X, Anderson ME, Ward A, Kung J. Image-guided core needle biopsy of adipocytic tumors: Diagnostic Accuracy and Concordance With Final Surgical Pathology. AJR Am J Roentgenol. 2021;216(4):997–1002.
57. Eizuru Y, Nakajo M, Nakajo M, Shinohara N, Yoshiura T. 18F-FDG PET/CT imaging of G-CSF-Producing Dedifferentiated Liposarcoma. Clin Nucl Med. 2022;47(1):e98–100.
58. Arthur A, Orton MR, Emsley R, Vit S, Kelly-Morland C, Strauss D, Lunn J, Doran S, Lmalem H, Nzokirantevye A, et al. A CT-based radiomics classification model for the prediction of histological type and tumour grade in retroperitoneal sarcoma (RADSARC-R): a retrospective multicohort analysis. Lancet Oncol. 2023;24(11):1277–86.
59. Tseng WW, Swallow CJ, Strauss DC, Bonvalot S, Rutkowski P, Ford SJ, Gonzalez RJ, Gladdy RA, Gyorki DE, Fairweather M, et al. Management of locally recurrent Retroperitoneal Sarcoma in the adult: an updated Consensus Approach from the Transatlantic Australasian Retroperitoneal Sarcoma Working Group. Ann Surg Oncol. 2022;29(12):7335–48.

Publisher's note